Simulation of Molecular Dynamics of Water Movement in Ion Channels

S. Kh. Aityan and Yu. A. Chizmadzhev

A. N. Frumkin Institute of Electrochemistry, Academy of Sciences of the USSR, Moscow 117071, USSR

Abstract. The motion of water molecules in a gramicidin-like channel was studied by the molecular dynamics method. Water molecules are presented in the ST2 model. The structure of the channel was presented in the form of channel's helix frame possessing mobile dipole groups. The interaction of all mobile particles with the membrane channel's walls was taken into account. The calculation consisted of 50,000 integration steps of $\Delta t = 5 \times 10^{-16}$ s which corresponded to a total elapsed time of 25 ps. It was shown that water molecules in the channel did not possess rigid spatial structure but exhibited a structure oriented along the channel axis. The motion of water molecules in the channel occurred smoothly, i. e. all water molecules did not have any deep, stable potential wells in the channel. The distribution of water molecules along the radial coordinate of the channel was estimated. Water density was shown to be maximal near the channel axis.

Key words: Molecular dynamics — Ion channels — Water — ST2 model

Introduction

Water plays an important role in the transport of ions through selective channels of biological and artificial membranes (Levitt et al. 1978; Rosenberg and Finkelstein 1978a, b). Direct measurements have shown that when potassium ions passed through gramicidin channels two to ten water molecules were transported per one potassium ion (Levitt et al. 1978), the stoichiometry entrainment coefficient being dependent on electrolyte concentration. Membrane permeability to water per se is of separate interest. However the way in which water behaves in channels; those respects in which it differs from bulk water and the manner in which it participates in the ion transport process are still to be elucidated. As shown by Rahman and Stillinger (1971) and Stillinger and Rahman (1974) bulk water molecules do not exhibit stable long-life states and behave like dynamic net. In contrast Fischer et al. (1981) and Fischer and Brickmann (1983) have demonstrated that a single ion transported in transmembrane channel exhibits quite stable long-life states inside

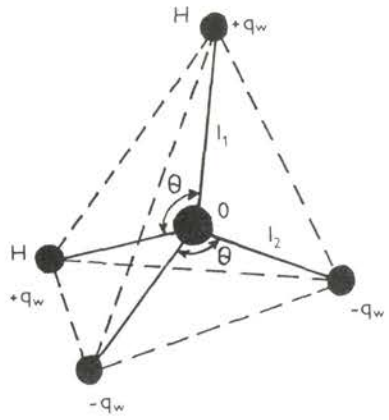

Fig. 1. The representation of water molecules in the ST2 model.

the channel because of its interaction with the channel frame. The present study was conducted to determine whether water molecules exhibit stable long-life state. In order to elucidate the dynamic structure of water in the channel, an analysis of various distribution and correlation functions as well as the water molecules trajectories within the channel was carried out.

The molecular dynamics method which has been successfully used to describe kinetic properties of bulk water (Rahman and Stillinger 1971; Stillinger and Rahman 1974), is apparently the most adequate procedure for solving the above problem. Following Stillinger and Rahman (1974) we used the ST2 model.

As the principal model for study we have chosen a model which possesses the main features of a gramicidin channel but, as discussed, contains some simplifications. The present choice is justifiable on the grounds that the gramicidin channel is studied most thoroughly so far, and its structure is relatively simple, though there are some controversies even over its structure (Bamberg et al. 1979; Weinstein et al. 1980; Sychev et al. 1980; Ivanov and Sychev 1982; Urry et al. 1983; Arseniev et al. 1984). This fact may provide an argument in favour of studying a simplified model. Such a channel had been already considered by Fischer et al. (1981) and Fischer and Brickmann (1983), who suggested that an ion may be presented in the channel's space, though the presence of water molecules was not taken into account. Besides, no consideration was given to ion interaction with the channel walls and a hydrophobic body of the membrane itself. In this paper we restrict ourselves to a discussion of water molecules motion in the model channel. The number of water molecules was chosen by fitting the value representing pressure at channel's edges.

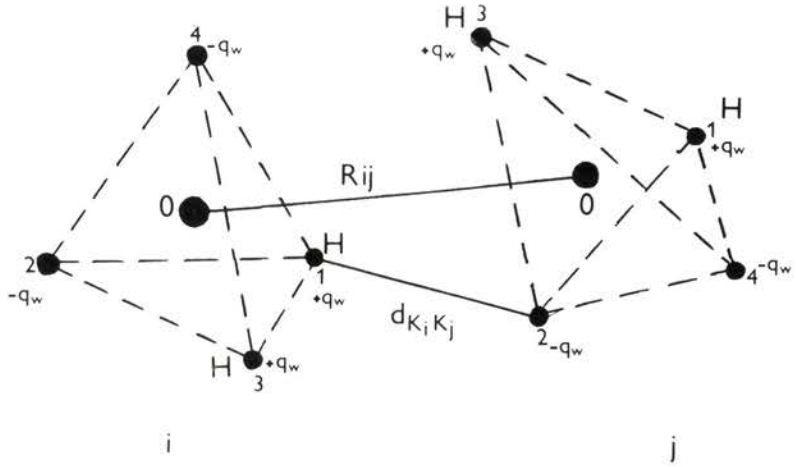

Fig. 2. The interaction of two model water molecules i and j. R_{ij} is the distance between oxygen atoms, $d_{k_i k_j}$ is the distance between the k_i apex of a model tetrahedron of molecule i and the k_j apex of a model tetrahedron of molecule j.

The model

As mentioned above, the water molecule is represented within the framework of the ST2 model (Stillinger nad Rahman 1974). In this model the water molecule was represented by a tetrahedron; at two apices the fixed charges q_w were located (corresponding to hydrogen atoms) and there were two fixed charges $(-q_w)$ located at the other two apices (corresponding to the spaced charge of oxygen atom). The ST2 model of water molecule is shown in Fig. 1, and parameters of this model are given below:

$$\begin{aligned} q_w &= 0.2357e \\ l_1 &= 0.1 \text{ nm} \\ l_2 &= 0.08 \text{ nm} \\ \Theta &= 109°28' = 2 \arccos(1/3) \\ m_H &= 1.6597\ 10^{-24} \text{ g} \\ m_O &= 2.6555\ 10^{-23} \text{ g} \end{aligned} \tag{1}$$

where e is the proton charge; l_1 is the distance from the oxygen atom to a hydrogen atom; l_2 is the distance from the oxygen atom to the apices of the tetrahedron carrying the charge $-q_w$; Θ is the angle between sections of a line connecting the oxygen atom with tetrahedron apices; m_H and m_O are masses of hydrogen and oxygen atoms, respectively.

According to the ST2 model, the potential of water-water interaction has the following form:

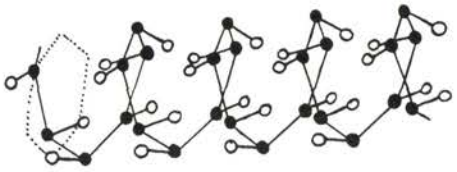

Fig. 3. The structure of a model channel frame (Fischer et al. 1981).

$$V_{ww}(i, j) = V_{ww}^{LJ}(R_{ij}) + S(R_{ij}) V_{ww}^{el}(i, j) \tag{2}$$

where indices i and j indicate two interacting molecules of water, R_{ij} is the distance between oxygen atoms of i and j molecules (Fig. 2), $V_{ww}^{LJ}(R)$ is the Lennard-Jones potential 6—12:

$$V_{ww}^{LJ}(R) = 4\varepsilon_{ww}[(\sigma_{ww}/R)^{12} - (\sigma_{ww}/R)^{6}] \tag{3}$$

where $\varepsilon_{ww} = 5.2605 \times 10^{-15}$ ergs,

$\sigma_{ww} = 0.31$ nm

V_{ww}^{el} is the Coulomb interaction potential of charged tetrahedron apices

$$V_{ww}^{el}(i, j) = q_w^2 \sum_{k_i, k_j = 1}^{4} (-1)^{k_i + k_j} / d_{k_i k_j} \tag{4}$$

$d_{k_i k_j}$ is the distance between the apex k_i of tetrahedron i and the apex k_j of tetrahedron j (Fig. 2), $S(R)$ is the modulating factor

$$S(R) = \begin{cases} 0 & 0 \leq R \leq R_L \\ \dfrac{(R - R_L)^2 (3R_u - R_L - 2R)}{(R_u - R_L)^3} & R_L < R < R_u \\ 1 & R_u \leq R \end{cases} \tag{5}$$

$R_L = 0.2016$ nm

$R_u = 0.31287$ nm

We specified the structure of the model channel based on the generalized structure of the gramicidin channel. The model channel (Fig. 3) contains mobile dipole groups structured in a hexagonal helix. The effective charge $\pm q_G$ being localized at two poles of these dipoles. The pole of the mobile dipole carrying the positive charge $+q_G$ is fixed (in space) at the helical frame of the channel (Fig. 3). The other pole with the negative charge $-q_G$ is free in space, so the mobile dipole, as a whole, can rotate round the fixed pole (in the model by Fischer et al. (1981) the mobile dipoles could oscillate in the plane passing through the fixed pole of the dipole and the geometric axis of the channel). The parameters of this system are as follows:

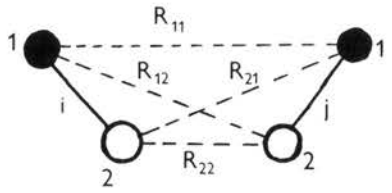

Fig. 4. The interaction of two mobile dipoles of a model channel. $R_{k_i k_j}$ is the distance between the k_i pole of mobile dipole i and the k_j pole of mobile dipole j.

$$
\begin{aligned}
q_G &= 0.2\ e \\
d &= 0.11\ \text{nm} \\
r_{ch} &= 0.3\ \text{nm} \\
h &= 1.2\ \text{nm} \\
D_r &= 1 \times 10^{-11}\ \text{ergs} \\
\varphi_o &= \pm 70^\circ
\end{aligned}
$$

where d is the dipole arm (the length of the C=O bond); r_{ch} is the radius of the helical channel's frame; D_r is the force constant of the dipole oscillations; φ_o is the angle which lays in the plane passing through the fixed pole of the dipole and the channel axis, and shows the equilibrium dipole deflection from plane perpendicular to the channel axis. The neighbouring dipoles have equilibrium angles of opposite sign. Each turn of the helix contains six mobile dipoles (Fig. 3).

The mobile dipoles of the helical frame interact between each other (Fig. 4) with a potential:

$$V_{GG}(i, j) = V_{GG}^{LJ}(i, j) + V_{GG}^{el}(i, j) \tag{7}$$

where $V_{GG}^{LJ}(i, j)$ is the Lennard-Jones potential, $V_{GG}^{el}(i, j)$ is the Coulomb interaction potential

$$
\begin{aligned}
V_{GG}^{LJ}(i, j) &= 4 \sum_{k_i, k_j = 1}^{2} \varepsilon_{GG}^{k_i k_j} \left[(\sigma_{GG}^{k_i k_j} / R_{k_i k_j})^{12} - (\sigma_{GG}^{k_i k_j} / R_{k_i k_j})^{6} \right] \\
V_{GG}^{el}(i, j) &= q_G^2 \sum_{k_i, k_j = 1}^{2} (-1)^{k_i + k_j} / R_{k_i k_j}
\end{aligned} \tag{8}
$$

Here $R_{k_i k_j}$ is the distance between k_i pole of mobile dipole i and k_j pole of mobile dipole j ($k_i = 1$ is the fixed pole with the effective charge q_G, $k_i = 2$ is the mobile pole with the effective charge $-q_G$). $\varepsilon_{GG}^{k_i k_j}$ was set as 5×10^{-15} ergs and $\sigma_{GG}^{k_i k_j}$ was set as 0.3 nm. Furthermore, every mobile dipole has additional potential energy connected with a deviation from the equilibrium dipole's position

$$V_G(\mathrm{i}) = \frac{1}{2} D_r \Delta\varphi^2 \tag{9}$$

where $\Delta\varphi$ is angular deflection from the equilibrium position.

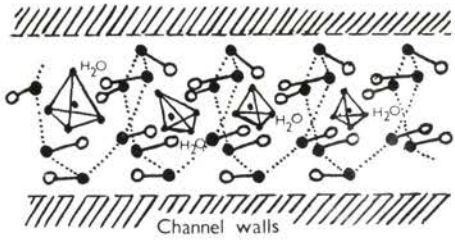

Fig. 5. The representation of a model channel with water molecules, built in the membrane.

The mobile dipoles of the helical frame of the channel also interact with water molecules inside the channel with the Lennard-Jones potential $V_{WG}^{LJ}(i, j)$ and the Coulomb potential $V_{WG}^{el}(i, j)$

$$V_{WG}(i, j) = V_{WG}^{LJ}(i, j) + V_{WG}^{el}(i, j) \tag{10}$$

where

$$V_{WG}^{LJ}(i, j) = 4 \sum_{k_j=1}^{2} \varepsilon_{WG}^{k_j} [(\sigma_{WG}^{k_j}/R_{ik_j})^{12} - (\sigma_{WG}^{k_j}/R_{ik_j})^{6}] \tag{11}$$

$$V_{WG}^{el}(i, j) = \sum_{k_i=1}^{4} \sum_{k_j=1}^{2} (-1)^{k_i+k_j}/d_{k_ik_j} \tag{12}$$

R_{ik_j} is the distance between an oxygen atom of a water molecule i and the k_j pole of a mobile dipole j of the helical frame of the channel, $d_{k_ik_j}$ is a distance between the k_i charged apex of a model tetrahedron of water molecule i and the k_j pole of the mobile dipole j. $\varepsilon_{WG}^{k_j}$ and $\sigma_{WG}^{k_j}$ are calculated from ε_{WW}, $\varepsilon_{GG}^{k_jk_j}$ and σ_{WW}, $\sigma_{GG}^{k_jk_j}$ by

$$\begin{aligned} \varepsilon_{WG}^{k_j} &= (\varepsilon_{WW} \cdot \varepsilon_{GG}^{k_jk_j})^{1/2} \\ \sigma_{WG}^{k_j} &= \frac{1}{2} (\sigma_{WW} + \sigma_{GG}^{k_jk_j}) \end{aligned} \tag{13}$$

Moreover, we have taken into account the presence of channel walls (Fig. 5) by introducing the potential of interaction between the wall and all mobile particles in a channel in a form of modulated Lennard-Jones repulsion potential

$$V_M = 4\varepsilon_M \left(\frac{r}{r_M - r}\right)^{12} \tag{14}$$

where r is the radial coordinate of the corresponding particle in a cylindrical channel space ($r_M > r_{ch}$). ε_M is chosen as 5×10^{-15} erg and r_M as 0.4 nm. We have chosen a potential V_M in the form of modulated repulsion potential (14) rather

than the conventional Lennard-Jones potential in order to avoid the step behaviour of interaction force at the channel axis.

All interactions given above completely determine the dynamic system which is described by the Hamilton system of equation

$$\dot{q}_i = \frac{\partial H}{\partial p_i}; \qquad \dot{p}_i = -\frac{\partial H}{\partial q_i} \tag{15}$$

where H is the total Hamiltonian of a system, p_i is a generalized momentum and q_i is a generalized coordinate of the system.

The model representation

The real system includes, besides the membrane, channel and particles, also the solutions which are separated by this membrane. In the molecular dynamics approach, the account for solutions makes the system far more complicated. In virtue of this fact, we considered an infinite channel in a membrane. It means, within the framework of molecular dynamics representation, that to the left and right sides of the channel there is an infinite series of periodic copies of the channel. Such a procedure has been implementes in molecular dynamics simulation of bulk water (Rahman and Stillinger 1971; Stillinger and Rahman 1974) and water solutions (Heinzinger et al. 1978) as well as in calculations of particles transport throught channels (Fischer et al. 1981; Aityan and Chizmadzhev 1982; Aityan 1983; Fischer and Brickmann 1983; Aityan and Chizmadzhev 1984).

However, the limitations of numerical calculations do not allow to take into account all periodic copies of the system and, hence, all interactions with these copies. Thus some interaction cutoff radius, R_C, was introduced in the system, such that all particles located at distances larger than R_C are considered to be non-interacting (Rahman and Stillinger 1971). If all interactions at distances $R > R_C$ are simply neglected (Rahman and Stillinger 1971) then at the distance $R = R_C$ the interaction would have a discontinuity, and this would give rise to instability of the first integral in the set of differential equations of motion resulting in a permanent rise of the system temperature (particle acceleration). To avoid this difficulty, it was proposed by Szasz and Heinzinger (1979) to re-normalize all forces and potentials in the system to eliminate the interaction discontinuity point. Let $F(R)$ and $V(R)$ be the values of interaction force and energy, respectively, as functions of a distance. (The vector of force $\vec{F}(R) = F(R)\frac{\vec{R}}{R}$). Then according to Heinzinger et al. (1978) and Szasz and Heinzinger (1979) we introduce new force

$$\vec{F}_N(R) = (F(R) - F(R_c))\frac{\vec{R}}{R}, \qquad R \leqslant R_c;$$
$$\vec{F}_N(R) = 0 \qquad , \qquad R > R_c \tag{16}$$

and potential

$$V_N(R) = V(R) + F(R_c)R + C, \qquad R \leqslant R_c$$
$$V_N(R) = 0 \qquad , \qquad R > R_c \tag{17}$$

where

$$C = -V(R_c) - F(R_c)R_c \tag{18}$$

Thus, for example, for the interaction of Coulomb type ($\sim 1/R^n$)

$$V(R) = \frac{A}{R^n}; \qquad \vec{F}(R) = \frac{nA}{R^{n+1}}\cdot\frac{\vec{R}}{R} \tag{19}$$

we have

$$\vec{F}_N(R) = nA\left(\frac{1}{R^{n+1}} - \frac{1}{R_c^{n+1}}\right)\frac{\vec{R}}{R}, \qquad R \leqslant R_c$$
$$\vec{F}_N(R) = 0 \qquad , \qquad R > R_c \tag{20}$$

and

$$V_N(R) = V(R) + nAR/R_c^{n+1} + C, \qquad R \leqslant R_c$$
$$V_N(R) = 0 \qquad , \qquad R > R_c \tag{21}$$

$$C = -V(R_c) - nA/R_c^n \tag{22}$$

The molecular dynamics simulation carried out in this study consists of three stages. Since in any similar simulation the system is generally "started" from initial conditions which may be arbitrarily specified, the initial configuration may have rather high interaction potential which might lead, by virtue of a finite step of integration, to the "explosion" of the system. To avoid these undesirable consequences, we introduced the first stage of calculation — the *evolution*; in essence means that all interactions are considered to be zero in the initial configuration and then rise up slowly to the required values.

The second stage was called *thermalization*. The essence of this stage consisted in bringing the system to a specified level of temperature. Since, within the framework of the approach, the closed system was considered, and its initial configuration was chosen arbitrarily, in the process of the system's aging all abundant potential energy of interaction would be "converted" into kinetic energy, and the temperature in the system would rise until it reaches some level of dynamic equilibrium. As is usual in similar simulations (Rahman and Stillinger 1971;

Stillinger and Rahman 1974; Heinzinger et al. 1978; Szasz and Heinzinger 1979; Fischer et al. 1981; Aityan and Chizmadzhev 1982, 1984; Aityan 1983), we calculated temperature according to the formula

$$T = \frac{\sum_{i=1}^{N_w} m\vec{v}_i\vec{v}_i + \sum_{i=1}^{N_w} \vec{\omega}_i^{\,\dagger} I_i^{w} \vec{\omega}_i + \sum_{i=1}^{N_G} \vec{\omega}_i^{G\dagger} I_i^{G} \vec{\omega}_i^{G}}{3k(2N_w + N_G)} \tag{23}$$

where k is the Boltzmann constant, T is the absolute temperature, N_w is the number of water molecules, N_G is the number of mobile dipoles, m is the mass of water particles, I_i^w and I_i^G are the tensors of moment of inertia of water molecule i and mobile dipole of the channel frame, respectively, $\vec{v}_i$ and $\vec{\omega}_i$ are the linear and angular velocities of water molecules, $\vec{\omega}_i^G$ is the angular velocity of dipole oscillations ($\vec{\omega}_i^{\,\dagger}$ and $\vec{\omega}_i^{G\dagger}$ are the transposed vectors).

The stage of system thermalization is aimed at bringing the system to the required level of temperature. The stage of thermalization consists of a periodic release of kinetic energy (zeroing all velocities), which leads a decrease in the system's temperature or re-normalizing velocities to fit the temperature at the required level. Since the number of particles in the system under consideration is limited, large fluctuations of temperature arise at each step of calculation. To avoid these large temperature fluctuations we have averaged the temperature of system (23) over several integration steps.

The third stage was called *run*. When this stage starts the system is already thermalized, and at the run stage all the required characteristics of the system are calculated.

In the accepted algorithm with the step of integration $\Delta t = 5 \times 10^{-16}$ s the stage of evolution required about 10^2 time steps, the stage of thermalization — about 10^4 steps, and the run stage lasted about 5×10^4 to 10^5 steps, requiring 8 to 16 hours of processor time for ECI060 computer.

Calculation technique

Using interaction potentials specified by Eqs. (2)—(5), (7)—(14), one may calculate all forces and torques acting on all mobile particles in the system. All types of translational motion in the system are described by the equation

$$m\ddot{x}_k = F_k \tag{24}$$

where m is the mass of the given particle, x is its coordinate, F is the force, index k indicates the corresponding component of vector ($k = 1, 2, 3$). The angular rotations are written down in the principal axes of inertia as

$$\begin{aligned} I_{x'}\dot{\omega}_{x'} + \omega_{y'}\omega_{z'}(I_{z'} - I_{y'}) &= M_{x'} \\ I_{y'}\dot{\omega}_{y'} + \omega_{z'}\omega_{x'}(I_{x'} - I_{z'}) &= M_{y'} \\ I_{z'}\dot{\omega}_{z'} + \omega_{x'}\omega_{y'}(I_{y'} - I_{x'}) &= M_{z'} \end{aligned} \tag{25}$$

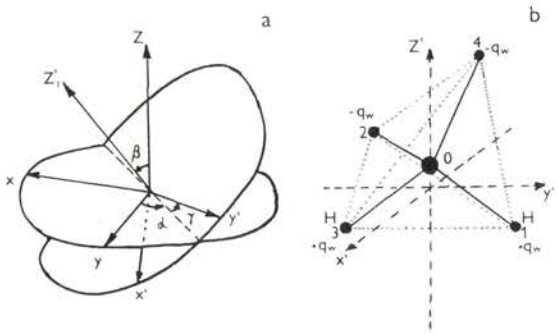

Fig. 6. *a*) Euler angles of coordinate system rotation; *b*) Body (mobile) coordinates of a model water molecule.

where $I_{x'}$, $I_{y'}$, $I_{z'}$, are the principal moments of inertia; $\omega_{x'}$, $\omega_{y'}$, $\omega_{z'}$ are angular velocities in body (mobile) axes coinciding with principal axes of inertia; $M_{x'}$, $M_{y'}$, $M_{z'}$ are torques relative to mobile axes.

To determine the spatial orientation of water molecules we made use of the Euler angles α, β, γ (Fig. 6). However as mentioned by Heinzinger et al. (1978) the direct use of the Euler angles in numerical calculations makes the system nonconservative, i. e. the total energy of the system is permanently growing. Besides, in this representation the inverse transformation

$$\begin{aligned}
\omega_{x'} &= \dot{\alpha} \sin \beta \cos \gamma + \dot{\beta} \sin \gamma \\
\omega_{y'} &= \dot{\alpha} \sin \beta \sin \gamma + \dot{\beta} \cos \gamma \\
\omega_{z'} &= \dot{\alpha} \cos \beta + \dot{\gamma}
\end{aligned} \tag{26}$$

has a singularity at $\beta = 0$. The above difficulties are overcome to a considerably degree, if the Euler angles (α, β, γ) are replaced by quaternion parameters (ξ, η, ζ, χ)

$$\begin{aligned}
\xi &= -\sin \frac{\beta}{2} \cos \frac{(\alpha - \gamma)}{2} \\
\eta &= -\sin \frac{\beta}{2} \sin \frac{(\alpha - \gamma)}{2} \\
\zeta &= \cos \frac{\beta}{2} \sin \frac{(\alpha + \gamma)}{2} \\
\chi &= \cos \frac{\beta}{2} \cos \frac{(\alpha + \gamma)}{2}
\end{aligned} \tag{27}$$

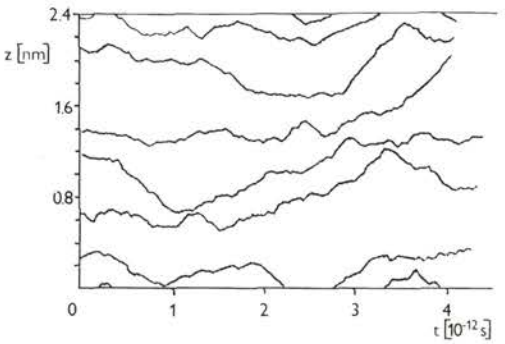

Fig. 7. Trajectories of the motion of water molecules along the channel axis.

Then the equation (26) takes the form

$$\begin{pmatrix} \omega_{x'} \\ \omega_{y'} \\ \omega_{z'} \\ 0 \end{pmatrix} = 2 \begin{pmatrix} -\zeta & \chi & \xi & -\eta \\ -\chi & -\zeta & \eta & \xi \\ \eta & -\xi & \chi & -\zeta \\ \xi & \eta & \zeta & \chi \end{pmatrix} \begin{pmatrix} \dot{\xi} \\ \dot{\eta} \\ \dot{\zeta} \\ \dot{\chi} \end{pmatrix} \tag{28}$$

which is regular for all values of the Euler angles.

To integrate the dynamics equations numerically we used the predictor-corrector method described by Gear (1966). The advantage of this method is that, along with high-speed operation (the method calls for the right-hand side of the differential equation only once at each step of integration), it possesses high accuracy at rather high integration step. The advantages of the predictor-corrector method are described in detail by Heinzinger et al. (1978). In present study we have used the predictor-corrector method of the fifth order to solve the equations of translational motion and an equivalent method of the seventh order to solve the equation of rotational motion. The step of integration $\Delta t = 5 \times 10^{-16}$ s has been chosen by computer experimentation. In this implementation, at the run stage 50,000 steps were done, which is equivalent to the total elapsed time of 2.5×10^{-11} s = 25 ps. The temperature of the system was 500°K, and the drift of the total energy corresponded to the stability of temperature varied within the limits of 6%.

Results

When implementing the molecular dynamics method described above, we have assumed that three water molecules correspond to each helix turn of the channel frame. Two helix turns were taken as the basic sections of the channel.

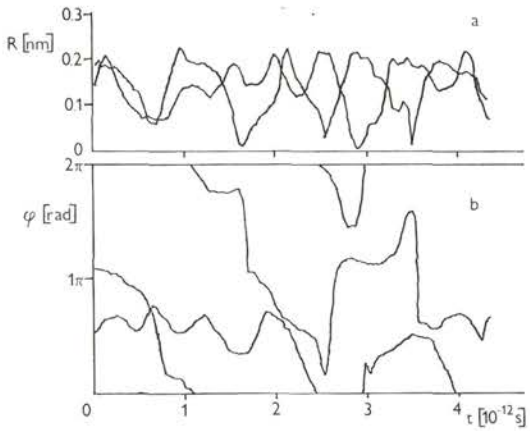

Fig. 8. Trajectories of the motion of water molecules along the radial (*a*) and angular (*b*) coordinates of the channel.

(i) Trajectories of motion

The obtained trajectories for the motion of water molecules inside the channel are represented in cylindrical coordinates of the channel. As an example, Fig. 7 shows trajectories for the motion of water molecules along the channel axial coordinate, and Fig. 8 shows similar trajectories along the radial and angular coordinates of the channel. The points of localization of particles on the trajectory in Figs. 7 and 8 are shown at every 5×10^{-14} s, i. e. in each of the 100 integration steps. The trajectories, shown in this figure, cover a time interval of 4 ps. It is evident from Fig. 7 that in the process of motion inside the channel the trajectories of water molecules along the axial coordinate of the channel are smooth enough, i.e. when moving along the channel, water molecules do not have prominent localized positions (potential wells), where they would exist for sufficiently long periods of time, sometimes jumping between the wells as in the case of transport of single ion (Fischer et al. 1981; Fischer and Brickmann 1983). It may be seen from Fig. 8 that water molecules, when passing through the channel, rapidly move along the radial an angular coordinates of the channel. This motion resembles oscillatory or spiral motion.

(ii) Distribution over the radial coordinate of the channel

Fig. 9*a* shows the distribution of water molecules over the radial coordinate of the channel. The figure shows that water molecules are mainly localized in the middle of the channel radius, rather than at the axis ($r = 0$), or at the channel walls ($r = r_{ch}$), and this effect exhibits the specific character of channel-forming groups

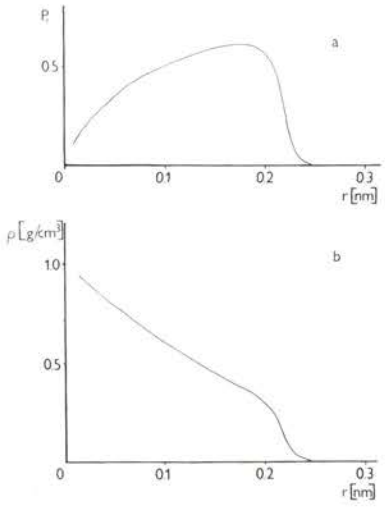

Fig. 9. *a*) The distribution of water molecules over the radial coordinate of the channel; *b*) The dependence of water density on the radial coordinate of the channel.

interaction with water molecules. The channel's radial coordinate distribution function $P_r(r)$ (Fig. 9*a*) can be interpreted as the dependence of water bulk density $\varrho(r)$ on the radial coordinate of the channel (Fig. 9*b*).

$$\varrho(r) = \frac{N_w m_w}{2\pi r l_{ch}} P_r(r) \tag{29}$$

where l_{ch} is the channel length. Figure 9*b* shows that the bulk microdensity of water is maximal near the channel axis. The apparent discrepancies between Figs. 9*a* and 9*b* disappear if one remembers that the $\varrho(r)$ function is obtained from $P_r(r)$ normalized with respect to $1/2\pi r$. Thus, even a minimal quantity of water molecules near the channel axis provide high bulk density.

(iii) The spatial correlation function

Fig. 10 illustrated spatial pair correlation function for water molecules along the axial coordinate of a channel

$$P_{zz}(|z_1 - z_2|) = \int P(\vec{R}_1, \vec{R}_2)\, d\vec{R}_1 d\vec{R}_2 \tag{30}$$
$$|z_1 - z_2| = \text{const}$$

where $\vec{R} = (x, y, z)$, and $P(\vec{R}_1, \vec{R}_2)$ is a pair state function of water molecules in the channel. In Fig. 10 the pair correlation function $P_{zz}(|z_1 - z_2|)$ has only two quite

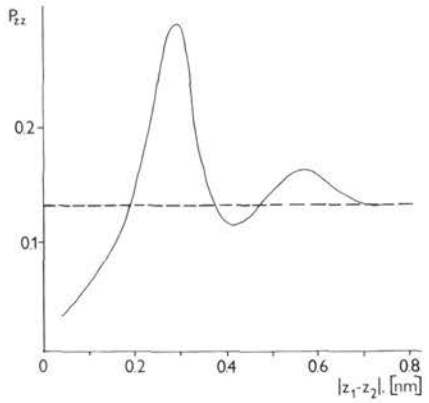

Fig. 10. The spatial pair correlation function for water molecules along the axial coordinate of the channel.

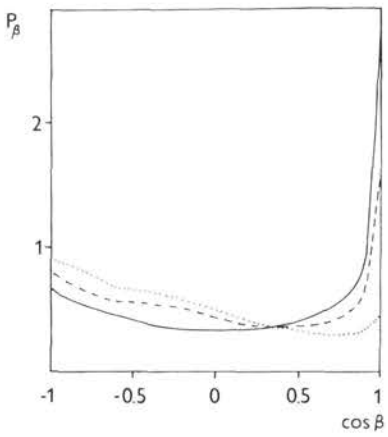

Fig. 11. The orientation distribution of water molecules after: 1000 steps (dotted line), 10,000 steps (dashed line) and 50,000 steps (solid line).

pronounced peaks: the second peak being smaller than the first one. Any subsequent peaks are hardly pronounced within the accuracy of avereging which indicates the absence of strong long-range correlations of long-range water structure in the channel.

(iv) The spatial orientation of water molecules

Fig. 11 shows the function depicturing the distribution of the orientation of water

molecules, $P_\beta(\cos\beta)$, which describes the deviation of the water molecular axis from the channel axis. As the figure shows, the water molecules are oriented mainly along the channel axis. Fig. 11 shows for comparison these distribution functions, $P_\beta(\cos\beta)$, after 1,000 time steps, that corresponds to 5×10^{-13} s (dotted line), 10,000 steps — 5×10^{-12} s — (dashed line) and 50,000 steps — 2.5×10^{-11} s — (solid line). We should note that distribution curves, $P_\beta(\cos\beta)$, were already stabilized after 25,000 steps and did not change appreciably in a further run of up to 50,000 steps. The comparison of these figures shows that the arbitrary initial distribution of water molecules (the dotted line) transfers with time into the oriented distribution (the solid line). This fact indicates that water molecules in the channel tend to acquire a preferential spatial orientation along the channel axis.

Discussion

A molecular dynamics method was implemented to simulate the motion of water in a model transmembrane channel. 50,000 iterations with an integration time step of 5×10^{-16} s were performed in an algorithm implementation process. Thus the calculation covered a total elapsed time interval of 25 ps. This time interval was not long enough to study the passage of water molecules across the channel (the time required is about 10^{-7} s). However the time interval of 25 ps appeared to be sufficient to analyse water structure and to characterise the motion of water molecules within the transmembrane channel. In fact, by up to 50,000 time steps the main characteristics of the system were practically stable. The distribution function of the orientation of water molecules, $P_\beta(\cos\beta)$, (Fig. 11) appeared to stabilize after 25,000 time steps. The stabilization of the distribution function over the radial coordinate, $P_r(r)$, and the radial dependence of water density, $\varrho(r)$, shown in Fig. 9 (a, b) required 50,000 time steps. The stabilization of the pair correlation function, $P_{zz}(|z_1-z_2|)$, (Fig. 10) in this run occurred only with an accuracy of 20 per cent. These facts are consistent with the proposal that in a run of 50,000 time steps which corresponded to 25 ps equilibrium has been completely reached for translational motion over the radial coordinate ($P_r(r)$ and $\varrho(r)$) but not yet for the axial coordinate ($P_{zz}(|z_1-z_2|)$) because of the specific radius and the length of the channel are, proportionally, 3:24. Thus the characteristic time of reaching the translational equilibrium in the channel may be $10^{-11}\div10^{-10}$ s which corresponded to the evaluation by thermal velocities of water molecules. The characteristic time for reaching orientational equilibrium determined by rotational velocities of water molecules, and so the equilibration in this degree of freedom of the system was much shorter.

Data obtained from the molecular dynamics run yielded useful information concerning the character of water motion within the channel. As Fig. 7 shows, water molecules in the transmembrane channel did not have explicit long-life states

but were moving along quite smooth trajectories. It is notable that the same type of motion has been pointed out previously by Stillinger and Rahman (1974) in a molecular dynamics simulation of bulk water. Simultaneously the water molecules exhibited some motion along the radial and angular coordinates of the channel (Fig. 8). This was quite clear because the water molecules were moving along potential "ravines" formed by the mobile dipoles of the channel frame. However, in relation to their motion along the radial coordinate of the channel, the water molecules were distributed mainly at specific distances from the channel axis ($0.1 \div 0.2$ nm at a channel radius of 0.3 nm) as it is evident from the data of Fig. 9 *a*. Nevertheless, water material density at the channel axis was higher than at the distance about $0.1 \div 0.2$ nm from it. The radial distribution function, $P_r(r)$, shown in Fig. 9*a* describes the probability density of the location of a water molecule at a distance, r, from the channel axis. To convert this distribution function, $P_r(r)$, to water density, $\varrho(r)$, it is necessary to take the number of water molecules in the unit volume into account which leads to monotonically decreasing dependence of water density, $\varrho(r)$, on channel radius with $\varrho(r)$ being equal to 1 g/cm^3 at the channel axis (Fig. 9*b*).

As the water molecules possess a dipole moment and are in a narrow channel their structure takes a preferential orientation along the channel axis (Fig. 11). This water structure is considerably different from that exhibited in a bulk state. In spite of such an orientational structure, water in the channel remains in liquid state which is illustrated by the spatial pair correlation function, $P_{zz}(|z_1 - z_2|)$, in Fig. 10 with only two quite pronounced peaks. This fact indicates the absence of a longe-range correlation between the water molecules.

Acknowledgments. The authors wish to thank V. I. Portnov for assistance in the work and Prof. Dr. K. Heinzinger (Mainz, FRG) for fruitful discussion concerning energy stabilization methods in a system.

References

Aityan S. Kh. (1983): Transport through narrow pores. Abstracts of Contributions to International School on the Physics of Ionic Solvation, Lvov, p. 114

Aityan S. Kh., Chizmadzhev Yu. A. (1982): Molecular dynamics study of transport process in ion channels of biomembranes. Abstracts of 33-th Meeting IEO, Lyon

Aityan S. Kh., Chizmadzhev Yu. A. (1984): A molecular dynamics study on water molecule movement in ionic channel. Biologicheskiye Membrany **1**, 901—912 (in Russian)

Arseniev A. S., Barsukov I. L., Sychev S. V., Bystrov V. F., Ivanov V. T., Ovchinnikov Yu. A. (1984): Double helical conformation of gramicidin A. Bioiogicheskiye Membrany **1**, 5—17 (in Russian)

Bamberg E., Alpes H., Apell H.-J., Bradley R., Harter B., Quelle M.-J., Urry D. W. (1979): Formation of ionic channels in black lipid membranes by succinic derivatives of gramicidin A. J. Membrane Biol. **50**, 257—270

Fischer W., Brickmann J. (1983): Ion-specific diffusion rates through transmembrane protein channels. A molecular dynamics study. Biophys. Chem. **18**, 323—337

Fischer W., Brickmann J., Läuger P. (1981): Molecular dynamics study of ion transport in transmembrane protein channels. Biophys. Chem. **13,** 105—116

Gear C. W. (1966): The numerical integration of ordinary differential equations of various orders. Argonne National Laboratory Report, No. 7126

Heinzinger K., Riede W. O., Schaefer L., Szasz Gy. I. (1978): Molecular dynamics simulations of liquids with ionic interactions. In: "Computer Modeling of Matter" (Ed. P. Lykos), ACS Symp. Series, vol. 86, p. 1—28

Ivanov V. T., Sychev S. V. (1982): The gramicidin A story. In: Biopolymer Complexes (Ed. Snatzke G. and Bartmann W.), pp. 107—125, J. Wiley, New York

Levitt D. G., Elias S. R., Hautman J. M. (1978): Number of water molecules coupled to the transport of sodium, potassium and hydrogen ions via gramicidin, nonactin or valinomycin. Biochem. Biophys. Acta **512,** 436—451

Rahman A., Stillinger F. H. (1971): Molecular dynamics study of liquid water. J. Chem. Phys. **55,** 3336—3359

Rosenberg P. A., Finkelstein A. (1978a): Interaction of ions and water in gramicidin A channels. J. Gen. Physiol. **72,** 327—340

Rosenberg P. A., Finkelstein A. (1978b): Water permeability of gramicidin A-treated lipid bilayer membrane. J. Gen. Physiol. **72,** 341—350

Stillinger F. H., Rahman A. (1974): Improved simulation of liquid water by molecular dynamics. J. Chem. Phys. **60,** 1545—1557

Sychev S. V., Nevskaya N. A., Jordanov St., Shepel E. N., Miroshnikov A. I., Ivanov V. T. (1980): The solution conformation of gramicidin A and its analogs. Bioorgan. Chem. **9,** 121—151

Szász Gy. I., Heinzinger K. (1979): A molecular dynamics study of aqueous solutions. VIII. Improved simulation and structural properties of a NH_4Cl solution. Z. Naturforsch., **34,** 840—849

Urry D. W., Shaw R. G., Trapane T. L., Prasad K. U. (1983): Infrared spectra of the gramicidin A transmembrane channel: the single stranded-β^c-helix. Biochem. Biophys. Res. Com. **114,** 373—379

Weinstein S., Wallace B. A., Morow J. S., Veatch W. R. (1980): Conformation of the gramicidin A transmembrane channel: a ^{13}C nuclear magnetic resonance study of ^{13}C-enriched gramicidin in phosphatidylcholine vesicles. J. Membrane Biol. **143,** 1—19

Received April 9, 1984/Accepted November 11, 1985